European Polymer Journal 72 (2015) 12–22

Contents lists available at ScienceDirect

European Polymer Journal

journal homepage: www.elsevier.com/locate/europolj

Self-healing poly(N-isopropylacrylamide) hydrogels

Umit Gulyuz, Oguz Okay *

Istanbul Technical University, Department of Chemistry, 34469 Istanbul, Turkey

ARTICLE INFO

Article history:
Received 31 July 2015
Received in revised form 31 August 2015
Accepted 3 September 2015
Available online 6 September 2015

Keywords:
Poly(N-isopropylacrylamide)
Hydrogels
Self-healing
Temperature sensitivity
Hydrophobic associations
Mechanical properties

ABSTRACT

Substitution the covalently crosslinked polymer chains by supramolecular ones is a promising strategy to design self-healing hydrogels. Approaches for the synthesis of supramolecular poly(N-isopropylacrylamide) (PNIPAAm) hydrogels with the ability to self-heal are rare because of the bulky side groups of the polymer hindering formation of strong cooperative secondary interactions. Herein, we describe, for the first time to our knowledge, preparation of PNIPAAm hydrogels with autonomous self-healing ability. Strong hydrophobic interactions were used to physically crosslink PNIPAAm chains in a micellar solution. The hydrogels were prepared by micellar copolymerization of N-isopropylacrylamide (NIPAAm) with 2 mol% stearyl methacrylate (C18) in 0.25 M NaBr solution of cetyltrimethylammonium bromide (CTAB). The physical gels exhibit frequency-dependent dynamic moduli and a loss factor above 0.1 due to the temporary nature of the hydrophobic associations in the presence of surfactant micelles. Cyclic mechanical tests show significant mechanical hysteresis and reversible loading/unloading cycles up to large maximum strains indicating that the damage done to the gel samples during the loading is recoverable in nature. The hydrogels indeed have autonomous self-healing ability with an efficiency of up to 100%. After swelling in water, the hydrogels undergo a significant change in their internal dynamics and lose their ability to self-heal due to the strengthening of hydrophobic associations in the absence of CTAB. By incorporating acrylic acid (AAc) units within the supramolecular PNIPAAm network, self-healing in swollen PNIPAAm hydrogels is achieved due to the fixing of CTAB in the gel phase by complexation with AAc units.

1. Introduction

Poly(N-isopropylacrylamide) (PNIPAAm) hydrogel is a classical temperature-sensitive gel exhibiting a volume phase transition at approximately 34 °C [1,2]. Below this temperature, the gel is swollen while it shrinks as the temperature is raised due to the conformational transition of PNIPAAm chains from coil to globule. The temperature sensitivity of PNIPAAm hydrogels has attracted great attention in the past years due both to fundamental and technological interests [3–10]. These materials are useful for drug delivery systems, separation operations in biotechnology, processing of agricultural products, sensors, and actuators. However, an obvious limitation of PNIPAAm hydrogels is their poor mechanical performance in swollen state. In many applications, self-healing is also crucial to enhance the lifetime of such soft and non-biodegradable materials.

* Corresponding author.
E-mail address: okayo@itu.edu.tr (O. Okay).

http://dx.doi.org/10.1016/j.eurpolymj.2015.09.002
0014-3057/

Inspired by the natural processes such as blood clotting or repairing of fractured bones [11–13], several techniques have been developed in recent years to create synthetic materials with self-healing abilities [14–21]. Substitution the covalently crosslinked polymer chains by supramolecular ones is a promising strategy to design self-healing hydrogels [22–24]. Different reversible molecular interactions have been used in the past few years to generate self-healing in synthetic hydrogels, including hydrogen bonding [25–27], electrostatic interactions [28], molecular recognition [29], metal coordination [30], $\pi-\pi$ stacking [31], dynamic chemical bonds [32], molecular diffusion [33], and hydrophobic associations [34]. Approaches for the preparation of self-healing PNIPAAm hydrogels are rare because of the bulky side groups of PNIPAAm chains hindering formation of strong cooperative secondary interactions [27,35]. Supramolecular PNIPAAm chains and networks have been synthesized by metal–ligand coordination [36], host–guest complexes [37], and H-bonding or metal-complexing side groups [38]. Haraguchi et al. showed that, although nanocomposite hydrogels based on pol(N,N-dimethylacrylamide) show self-healing properties, those based on PNIPAAm hardly self-heal even at 50–80 °C [27]. In a follow-up study, Wang et al. prepared similar hydrogels but using acrylamide (AAm) and N-isopropylacrylamide (NIPAAm) copolymer instead of PNIPAAm homopolymer [35]. They showed that self-healing efficiency decreases as the NIPAAm content of the copolymer increases and pure nanocomposite PNIPAAm gels have autonomous self-healing efficiency of less than 20%.

We recently presented a simple strategy to create self-healing hydrogels consisting of hydrophobically modified hydrophilic polymers and wormlike micelles [34,39–44]. Large hydrophobes such as stearyl methacrylate (C18) could be copolymerized with hydrophilic monomers in a micellar solution of surfactants such sodium dodecyl sulfate (SDS), or cetyltrimethylammonium bromide (CTAB). This was achieved by the addition of salt into the reaction solution [39]. Salt leads to micellar growth and thus enables solubilization of large hydrophobes within the grown wormlike surfactant micelles. After their solubilization and, after incorporation of the hydrophobic sequences within the hydrophilic polymer chains via micellar polymerization technique, strong hydrophobic interactions can be generated in synthetic hydrogels. Mixed micelles acting as physical crosslinks in such hydrogels are formed by dynamic hydrophobic association of the hydrophobic domains of hydrophilic polymer chains and grown surfactant micelles [40]. Hydrogels formed via such hydrophobic interactions in micellar solutions exhibit unique properties such as a high stretchability, high mechanical strength, along with complete autonomous self-healing [43,44].

Here, we report, for the first time to our knowledge, preparation of PNIPAAm hydrogels with autonomous self-healing ability. We prepared physical PNIPAAm hydrogels by copolymerization of NIPAAm with 2 mol% C18 in aqueous CTAB – NaBr solutions via micellar polymerization technique. As will be seen below, the physical PNIPAAm hydrogels formed in the micellar solution exhibit frequency-dependent dynamic moduli and a loss factor above 0.1, indicating temporary nature of the hydrophobic associations. Cyclic mechanical tests show significant mechanical hysteresis and reversible loading/unloading cycles up to large maximum strains indicating that the damage done to the gel samples during the loading is recoverable in nature. Indeed, the hydrogels have autonomous self-healing ability as evidenced by mechanical measurements. However, the hydrogels undergo a significant change in their internal dynamics upon swelling in water and lose their ability to self-heal. This structural change occurs due to the extraction of surfactant micelles from the gel network. By incorporating acrylic acid (AAc) units within the supramolecular PNIPAAm network, self-healing in PNIPAAm hydrogels in aqueous solutions is achieved due to the complexation between CTAB and AAc units in the gel phase.

2. Experimental

2.1. Materials

N-Isopropylacrylamide (NIPAAm, Aldrich) was recrystallized twice from benzene/hexane (35/65 v/v). Commercially available stearyl methacrylate (C18, Aldrich) consists of 65% *n*-octadecyl methacrylate and 35% *n*-hexadecyl methacrylate. Acrylic acid (AAc, Merck) was freed from its inhibitor by passing through an inhibitor removal column purchased from the Aldrich Chemical Com. Cetyltrimethylammonium bromide (CTAB, Sigma), ammonium persulfate (APS, Sigma–Aldrich), *N,N,N′,N′*-tetramethylethylenediamine (TEMED, Merck), α-ketoglutaric acid (Fluka), and sodium bromide (NaBr, Merck) were used as received. Stock APS solution was prepared by dissolving 0.8 g of APS in 10 mL of distilled water.

2.2. Hydrogel preparation

PNIPAAm hydrogels were prepared by the micellar copolymerization of NIPAAm with 2 mol% C18 at 25 °C in aqueous CTAB – NaBr solutions using APS (3.51 mM) – TEMED (0.25 v/v%) redox initiator system. CTAB and NaBr concentrations were fixed at 5 w/v% and 0.25 M, respectively. To illustrate the synthetic procedure, we give details for the preparation of PNIPAAm hydrogels at an initial monomer concentration C_o = 10 w/v%. CTAB (0.50 g) was dissolved in 8.5 mL aqueous solution of NaBr (0.2573 g) at 35 °C to obtain a transparent solution. Then, hydrophobic monomer C18 (0.0581 g) was dissolved in this CTAB–NaBr solution under stirring for 2 h at 35 °C. We have to mention that the hydrodynamic correlation length of 5 w/v% CTAB in water is 0.6 ± 0.1 nm, as compared to 6 ± 2 nm in 0.25 M NaBr [44]. This growth of CTAB micelles provides solubilization of C18 in the micellar solution. After addition and dissolving NIPAAm (0.9419 g) for 1 h, TEMED (25 μL) was added into the solution. Finally, 0.100 mL of APS stock solution was added to initiate the reaction. A portion of this solution was transferred between the plates of the rheometer to follow the reaction by oscillatory small-strain shear measurements.

For the rheological experiments with the hydrogels in swollen state, a portion of this solution was transferred between two glass plates (5 × 5 cm) separated by a 0.5 mm Teflon spacer. For the determination of the gel fraction and for the mechanical measurements, the remaining part of the solution was transferred into several plastic syringes of 4.7 mm internal diameters and the polymerization was conducted for 24 h at 24 °C. For comparison, micellar polymerization reaction of NIPAAm was also carried out in the absence of the hydrophobic comonomer C18. Poly(NIPAAm-AAc) hydrogels were prepared by micellar copolymerization of equimolar amounts of NIPAAm and AAc at 24 °C in aqueous CTAB–NaBr solutions. α-ketoglutaric acid (0.1 w/w% of the monomer solution) was added to initiate the reactions. The polymerization was conducted under UV lamp at a wavelength of 360 nm for 24 h.

2.3. Rheological experiments

Gelation reactions were carried out at 25 °C within the rheometer (Gemini 150 Rheometer system, Bohlin Instruments) equipped with a cone-and-plate geometry with a cone angle of 4° and a diameter of 40 mm. The instrument was equipped with a Peltier device for temperature control. During all rheological measurements, a solvent trap was used to minimize the evaporation. An angular frequency ω of 6.3 rad s^{-1} and a deformation amplitude γ_0 of 0.01 were selected to ensure that the oscillatory deformation is within the linear regime. After a reaction time of 2 h, the dynamic moduli of the reaction solutions approached limiting values. Then, frequency-sweep tests were carried out at 25 °C. The thermal behavior of the hydrogels was investigated by heating the gel samples between the parallel plates of the rheometer from 20 to 80 °C at a fixed rate of 2 °C/min. The changes in the dynamic moduli of gels were monitored during the course of the heating as a function of temperature at ω = 6.3 rad s^{-1} and γ_0 = 0.01.

2.4. Gel fraction and swelling measurements

Cylindrical hydrogel samples (diameter 4.7 mm, length about 2 cm) were immersed in a large excess of water at 24 °C for at least 15 days by replacing water every day to extract any soluble species. The mass m of the gel samples was monitored as a function of swelling time by weighing the samples. The relative mass m_{rel} of gels with respect to the after preparation state was calculated as $m_{rel} = m/m_0$, where m_0 is the initial mass of the gel sample. Then, the gel samples in equilibrium with pure water with a relative gel mass $m_{rel,eq}$ were taken out of water and freeze-dried. The gel fraction W_g, that is, the conversion of monomers to the cross-linked polymer (mass of water-insoluble polymer/initial mass of the monomer), was calculated from the masses of dry polymer network and from the comonomer feed.

2.5. Mechanical tests

Uniaxial compression and elongation measurements were performed on cylindrical hydrogel samples after synthesis (4.7 mm diameter) and after equilibrium in water in a thermostated room at 24 °C on a Zwick Roell test machine. Load and displacement data were collected during the experiments. The stress was presented by its nominal σ_{nom} or true values σ_{true} (= $\lambda.\sigma_{nom}$), which are the forces per cross-sectional area of the undeformed and deformed gel specimen respectively, while the strain is given by λ, the deformation ratio (deformed length/initial length). The fracture stress σ_f and the deformation λ_f at break were calculated from the maxima in σ_{true}–λ plots, as detailed previously [43]. The Young's modulus E was calculated from the slope of stress–strain curves between deformation of 5% and 15%. Uniaxial elongation measurements were performed using a 10 N load cell under the following conditions: cross-head speed = 50 mm min^{-1}; sample length between jaws = 11 ± 1 mm. Uniaxial compression measurements were performed using a 500 N load cell. Before the test, an initial compressive contact to 0.01 ± 0.002 N was applied to ensure a complete contact between the gel and the plates. Paraffin oil was used as lubricant to reduce friction and adhesion between the plates and the gel surface. Cyclic mechanical tests were conducted at a constant cross-head speed to a maximum elongation ratio, followed by retraction to zero force and a waiting time of 5 min, until the next cycle of elongation. The cross-head speed was 5 and 50 mm min^{-1} in compression and elongation, respectively. To quantify the healing efficiency, tensile testing experiments were performed using virgin and healed cylindrical gel samples of 4.7 mm diameter and 6 cm length. The virgin gel samples after synthesis and in equilibrium with water were cut in the middle, and then the two halves were merged together within a plastic syringe (of the same diameter as the gel sample) by slightly pressing the piston plunger.

3. Results and discussion

3.1. Hydrogels with surfactants

PNIPAAm hydrogels were prepared by micellar copolymerization of NIPAAm and the hydrophobic comonomer C18 in an aqueous CTAB–NaBr solution. C18 content of the comonomer feed was fixed at 2 mol% throughout this study. Preliminary experiments showed that the hydrogels formed at or below 5% NIPAAm were too weak while those formed above 20% had no autonomous self-healing ability. Therefore, the results obtained at initial monomer concentrations C_o of 10% and 15% (w/v) will be presented and discussed. We first monitored formation of PNIPAAm hydrogels by real-time rheological

measurements. In Fig. 1A, the elastic modulus G' (symbols) and the loss factor *tan* δ (= G''/G', lines) of the reaction solutions are shown as a function of the reaction time. The initial monomer concentrations C_o are 10% and 15% (w/v) as indicated in the figure. The general trend is a rapid increase of G' and decrease in *tan* δ during the first 30 min of the reaction time, followed by a plateau regime where they change only slightly. Control experiments conducted under the same reaction conditions but in the absence of C18 indicated that the hydrophobic comonomer is responsible for the significant increase in both the elastic and viscous, energy dissipating properties of the resulting physical gel system (Fig. S1). This reveals formation of intermolecular hydrophobic associations between the alkyl side chains of C18 units acting as physical crosslinks. Increasing monomer concentration C_o from 10% to 15% also increases the limiting elastic modulus while *tan* δ decreases indicating increasing elasticity of hydrogels (Fig. 1A).

After a reaction time of 2 h, frequency-sweep tests at $\gamma_o = 0.01$ were carried out over the angular frequency range 0.05–200 rad s^{-1}. Fig. 1B and C show the frequency (ω) dependencies of G' (filled symbols), the viscous modulus G'' (open symbols), and *tan* δ (lines) for the hydrogels formed at C_o = 10% and 15%, respectively. The gray symbols in Fig. 1B represent the dynamic moduli of PNIPAAm solution prepared under the same experimental condition except that C18 was not included into the comonomer feed. In the absence of C18, the system shows a liquid like response typical for a semi-dilute polymer solution, that is, G'' exceeds G' at low frequencies and there is a crossover frequency at 0.33 rad/s where the G' and G'' curves intersect. This situation drastically changes in the presence of the hydrophobic monomer C18. The crossover frequency shifts outside of the experimental window and simultaneously, both dynamic moduli assume higher values over all frequencies studied. The physical PNIPAAm hydrogels exhibit frequency-dependent dynamic moduli with a loss factor above 0.1 and thus, they belong to the category of weak gels. This is due to the temporary nature of the hydrophobic associations in the presence of surfactant micelles [40,43].

Temperature sensitivity of PNIPAAm hydrogels after their preparation state, i.e., in the presence of surfactant micelles was investigated by heating the gel samples prepared between the parallel plates of the rheometer from 20 to 80 °C at a rate of 2 °C/min. Fig. 2 shows G' (symbols) and *tan* δ (curves) of the hydrogels plotted against the temperature. Above 30 °C, the elastic modulus G' rapidly increases while the loss factor *tan* δ attains a minimum value at 33 °C, corresponding to the volume phase transition temperature. Similar changes in G' and *tan* δ were also observed in chemically crosslinked PNIPAAm hydrogels [45,46]. Another characteristic feature of the present hydrogels is the decrease of the modulus G' with rising temperature up to 30 °C (Fig. 2). Such as a decrease was not observed when C18 is not included in the system (Fig. S2) [46], indicating that the hydrophobic associations are responsible for this behavior. Previous work indeed shows that the modulus of semi-dilute solutions of hydrophobically modified polyacrylamides decreases with rising temperature below 30 °C [44,47,48]. This behavior is attributed to decreased lifetime of crosslinks and/or increased solubility of hydrophobic groups in aqueous solutions leading to a decrease in the association degree of polymers [47].

To determine the mechanical performance of the hydrogels, cylindrical gel samples after a reaction time of 24 h were subjected to uniaxial compression and tensile tests. Both during compression and elongation, the Young's modulus E of the hydrogels formed at C_o = 10% was found to be 5 ± 1 kPa while it increased to 20 ± 2 kPa upon increasing C_o to 15%. Solid curves in Fig. 3 represent stress–strain data of the hydrogels during compression ($\lambda < 1$) and elongation ($\lambda > 1$), as the dependence of the nominal stress σ_{nom} on the deformation ratio λ. The dashed curves were obtained from equilibrium swollen gel samples and will be discussed later. In elongation tests, the hydrogel formed at C_o = 10% sustains 18 ± 3 kPa stresses and ruptures at a stretch of 26 ± 5. Increasing C_o to 15% further increases the fracture stress to 49 ± 7 kPa while stretch at break decreases to 11 ± 2. The hydrogels are also mechanically stable up to 97% compressions.

Large strain properties of the hydrogels were investigated by cyclic compression and elongation tests. The tests were conducted by uniaxial deformation of cylindrical gel samples at a constant crosshead speed to a predetermined maximum load,

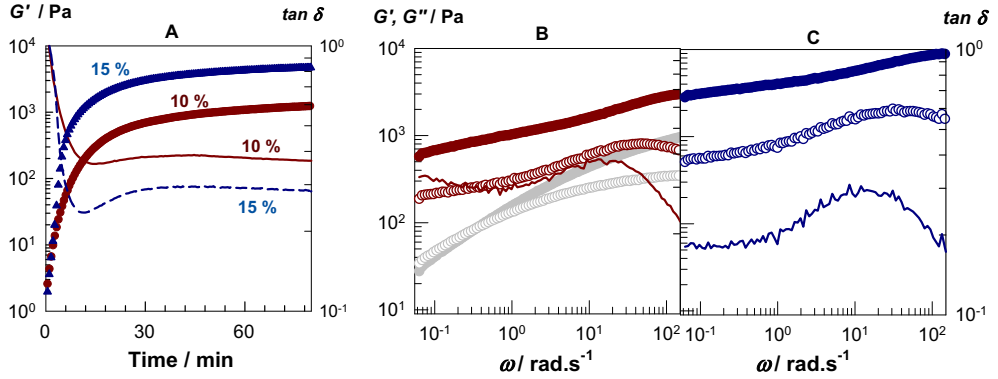

Fig. 1. (A): Elastic moduli G' (filled symbols) and the loss factor *tan* δ (lines) during the NIPAAm polymerization at 25 °C with 2 mol% C18 plotted against the reaction time. ω = 6.3 rad s^{-1} Initial monomer concentrations C_o indicated. (B and C): G' (filled symbols), the viscous modulus G'' (open symbols) and *tan* δ (lines) of the hydrogels at 25 °C shown as a function of angular frequency ω. C_o = 10% (B) and 15% (C). The filled and open gray symbols in B represent G' and G'' of PNIPAAm solution, respectively, obtained after the micellar polymerization of NIPAAm in the absence of C18. Reaction time = 2 h. $\gamma_o = 0.01$.

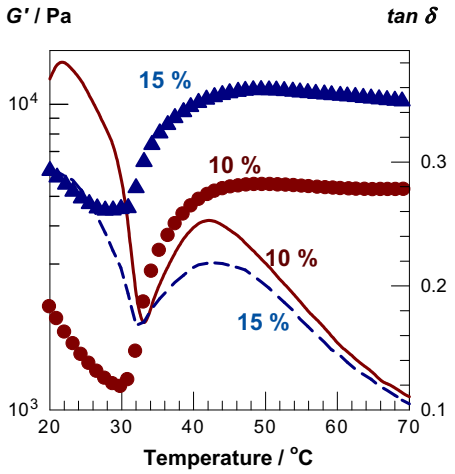

Fig. 2. G' (filled symbols) and *tan* δ (curves) of PNIPAAm hydrogels shown as a function of the temperature. $\omega = 6.3$ rad/s. $\gamma_o = 0.01$. C_0 as indicated.

followed by immediate retraction to zero displacement. After a fixed waiting time of 5 min, the cycles were repeated several times. In Fig. 4A and B, the true stress σ_{true} vs deformation ratio λ curves from three successive loading – unloading cycles up to a maximum compression of 90% ($\lambda_{max} = 0.1$) are shown for the hydrogels formed at $C_o = 10\%$ and 15%, respectively. It is seen that the loading curve of the compressive cycle is different from the unloading curve indicating dissipation of energy due to the damage in the gel sample. However, the behavior of virgin gel sample can be recovered when the sample is left to rest for 5 min without stress and subjected to repeated cycles. The area between the loading and unloading curves, corresponding to the hysteresis energy U_{hys}, is independent on the number of cycles and equals to 3 ± 0.3 and 7 ± 0.3 kJ m^{-3} for $C_0 = 10\%$ and 15%, respectively (see inset to Fig. 4A). The reversibility of loading/unloading cycles and good superposition of the successive loading curves demonstrate that the damage done to the gel samples during the loading is recoverable in nature.

Fig. 5A shows successive loading – unloading compression and tensile cycles of the hydrogels with increasing maximum strain. For clarity, loading and unloading curves of successive cycles are presented by the solid and dotted lines, respectively. Again, a good superposition of the successive loading curves demonstrates that the damage done to the gel samples during the loading cycle is self-repaired during the wait time between the cycles. The results also show that the energy associated with the hysteresis increases with increasing degree of deformation of the gel samples. Because the mechanical cycles are reversible, the hysteresis energy is due to the dynamic nature of hydrophobic associations that break and reform during loading and unloading, respectively. Since uniaxial compression is equivalent to biaxial stretching [49], we converted the maximum strain λ_{max} during compression to maximum biaxial extension ratio $\lambda_{biax,max}$ by $\lambda_{biax,max} = \lambda_{max}^{-0.5}$. In Fig. 5B, the energy U_{hys} dissipated during the compression and tensile cycles are plotted against the maximum strain in terms of uniaxial

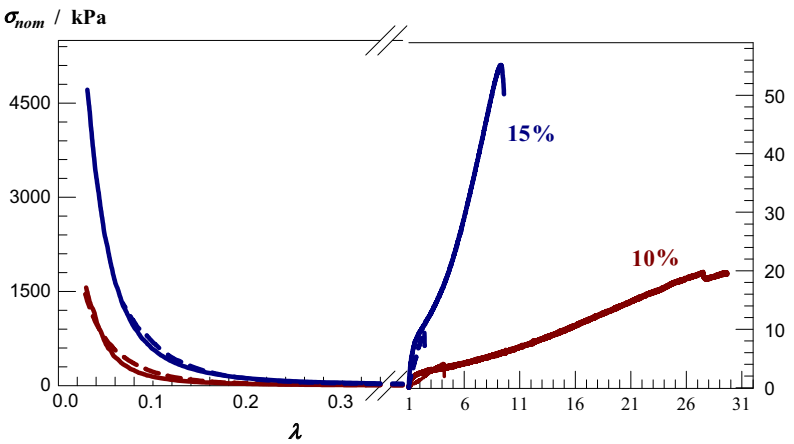

Fig. 3. Stress–strain curves of PNIPAAm hydrogels under compression ($\lambda < 1$) and elongation ($\lambda > 1$) as the dependence of nominal stress σ_{nom} on the deformation ratio λ. The solid and dashed curves represent data obtained from hydrogels just after preparation and after equilibrium swelling in water, respectively.

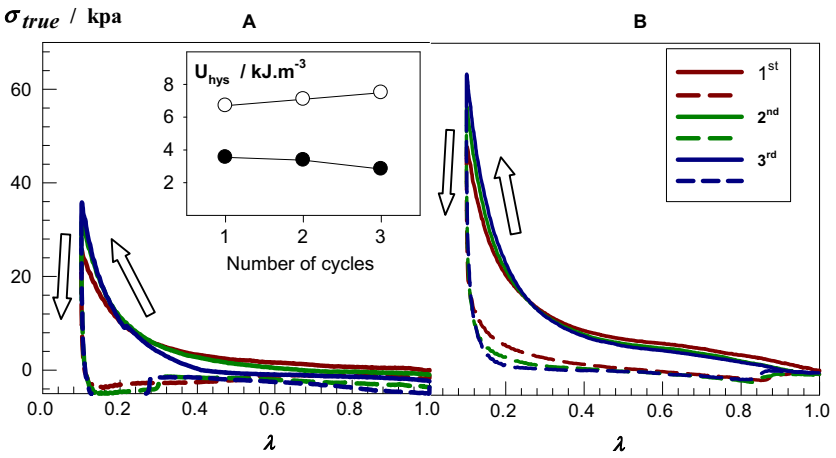

Fig. 4. True stress σ_{true} vs deformation ratio λ curves from cyclic compression tests for hydrogels formed at C_o = 10% (A) and 15% (B). Three successive loading/unloading cycles up to λ_{max} = 0.10 are shown. The inset to Fig. 1B shows the hysteresis energy U_{hys} plotted against the number of cycles for C_0 = 10% (filled symbols) and 15% (open symbols).

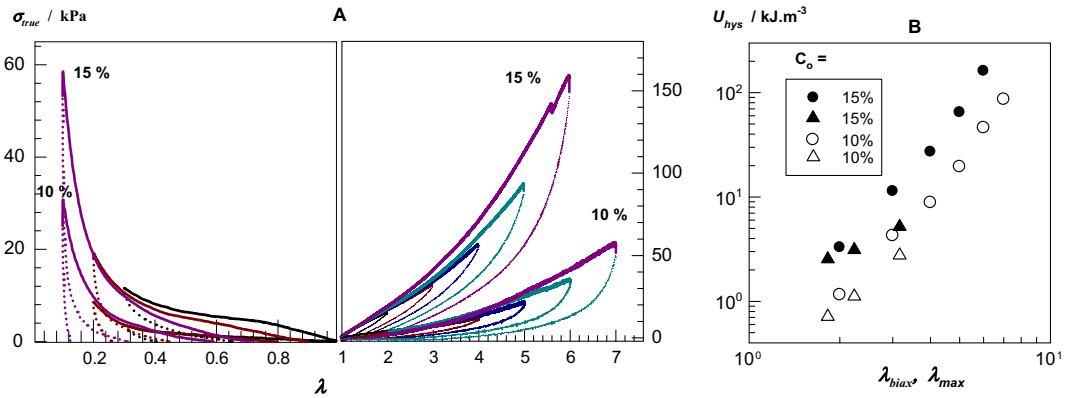

Fig. 5. (A): σ_{true} vs. λ curves of PNIPAAm hydrogels from cyclic compression ($\lambda < 1$) and elongation tests ($\lambda > 1$). The tests were conducted with increasing strain with a waiting time of 5 min between cycles. (B): Hysteresis energy U_{hys} during the loading/unloading compression (triangles) and elongation cycles (circles) of PNIPAAm hydrogels shown as a function of the maximum strain λ_{max} or $\lambda_{biax,max}$. C_o = 10% (open symbols) and 15% (filled symbols).

λ_{max} and biaxial extension ratios $\lambda_{biax,max}$. U_{hys} increases with increasing maximum strain during the loading step while it is almost independent on the type of deformation. Thus, the hysteresis energy only depends on the maximum extension of the polymer chains. Moreover, U_{hys} also increases with increasing C_o from 10% to 15%. This is due to the simultaneous increase of polymer concentration in hydrogels, so that more associations are reversibly broken under deformation leading to the release of greater amount of energy.

The result reveals reversible disengagements of the hydrophobic units from the associations under an external force and thus, preventing the fracture of PNIPAAm backbone. This also points out the self-healing ability of PNIPAAm hydrogels upon damage, which was indeed observed experimentally. As illustrated in Fig. 6A, when the fracture surfaces of ruptured PNIPAAm hydrogel samples are pressed together, the two pieces merge into a single piece. The joint reformed withstands large extension ratios before its fracture. To quantify the healing efficiency, tensile testing experiments were performed using virgin and healed cylindrical gel samples. The samples were cut in the middle and then, the two halfs were merged together at 24 °C for various healing times. In Fig. 6B, stress–strain curves of the virgin and healed gel samples formed at C_o = 10% and 15% are shown for different healing times. The modulus E could completely be recovered within 30 min indicating the occurrence of a rapid and autonomous self-healing process in the hydrogel. For the hydrogel formed at C_o = 10%, 30 min of healing time fully recover the mechanical performance of the virgin PNIPAAm hydrogel. The healing of the hydrogel formed at C_o = 15% requires longer times due to its higher elasticity. After 30 min, the fracture stress of the healed gel is 20 ± 2 kPa which is 35% of the fracture stress of the virgin sample. A healing time of 1 h increased the healing efficiency to 55 ± 5%.

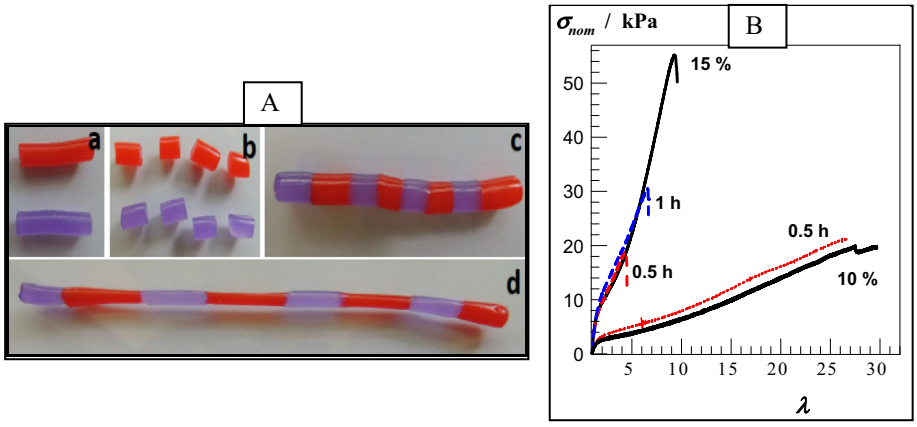

Fig. 6. (A): Photographs of virgin and healed PNIPAAm hydrogel samples formed at C_0 = 10%. The virgin gel samples are colored blue and red for clarity. Gel samples before (a) and after cutting into many pieces (b), after healing at 24 °C for 30 min (c), and after stretching (d). (B): Stress–strain curves of virgin (solid) and healed gel samples (dashed). Healing times are indicated. Temperature = 24 °C.

3.2. Hydrogels without surfactant

All the features of PNIPAAm hydrogels reported so far are related to their as-prepared state. Thus, the hydrogels contain surfactant micelles which may affect their physical properties. To characterize surfactant free hydrogels, gel samples were immersed in water at 24 °C for at least 15 days by replacing water every day to extract any soluble species. The gel fraction W_g was found to be 0.93 ± 0.04 and 0.97 ± 0.01 for C_o = 10% and 15%, respectively. This reveals that the monomers in the feed are almost completely converted into a water insoluble, physically crosslinked polymer network. Fig. 7A shows the swelling kinetic profiles of the hydrogels where the relative swelling ratio m_{rel} is plotted against the swelling time. m_{rel} first rapidly increases with the swelling time and, after passing a maximum, it decreases again to attain an equilibrium value $m_{rel,eq}$ of 3.4 ± 0.3 after 15 days. This swelling profile of PNIPAAm hydrogels is typical for gels containing ionic surfactants [40]. Thus, the hydrogel initially behaves like an ionic one and therefore, exhibits a large swelling ratio m_{rel} due to the osmotic pressure of CTAB counterions. As CTAB is progressively extracted from the gel, it gradually converts into a nonionic gel having a markedly reduced swelling ratio. The hydrogels equilibrium swollen in water also exhibited temperature sensitivity. As seen in the photographs (Fig. 7C), at 24 °C the physical gel is swollen; at 50 °C, the gel is collapsed. Fig. 7B showing the normalized swelling ratio m_{norm} of the hydrogels in water at various temperatures reveals that they undergo a deswelling transition at 33–34 °C, as reported for chemically crosslinked PNIPAAm gels [1,2,10]. Thus, incorporation of 2 mol% C18 units in PNIPAAm chains does not affect its transition temperature.

Fig. 8A and B show the frequency dependencies of G' (black symbols) and *tan* δ (black lines) for the equilibrium swollen PNIPAAm hydrogels formed at C_o = 10% and 15%, respectively. For comparison, the data obtained from the as-prepared hydrogels are also shown by gray symbols and lines. In contrast to the frequency-dependent modulus of the hydrogels after

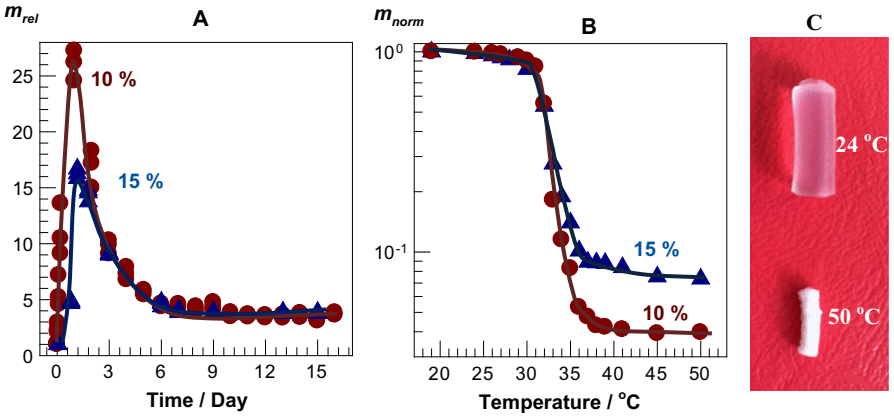

Fig. 7. (A): Relative mass m_{rel} of PNIPAAm hydrogels plotted against the swelling time in water. (B): The mass m_{norm} of the hydrogels equilibrium swollen in water plotted against the temperature. The mass of the gel is normalized with respect to its mass at 24 °C. C_o = 10% (circles) and 15% (triangles). (C): Photographs of the PNIPAAm physical gels at 24 and 50 °C. C_o = 10%.

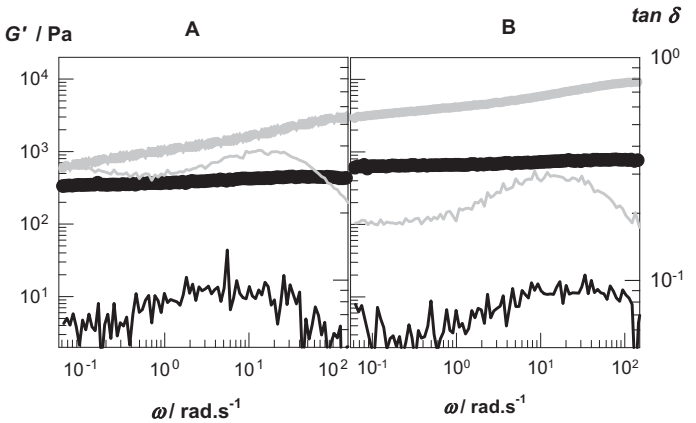

Fig. 8. G' (symbols) and *tan* δ (lines) of as-prepared PNIPAAm gels (gray) and gels after equilibrium swelling in water (black) shown as a function of angular frequency ω. C_o = 10% (A) and 15% (B). Temperature = 25 °C. γ_o = 0.01.

preparation state, the modulus G' of swollen hydrogels becomes nearly frequency independent. Moreover, the loss factor decreases from above to below 0.1 indicating weak-to-strong gel transition upon swelling in water. This reveals that the removal of surfactant micelles from the gel network strengthens the hydrophobic associations between the hydrophobic blocks due to their direct exposure to the aqueous environment [40]. Consequently, swollen PNIPAAm hydrogels behave similar to the chemically crosslinked ones.

The significant change in the internal dynamics of PNIPAAm hydrogels upon their swelling in water was also observable by cyclic mechanical tests. The cylindrical gel samples in equilibrium with water were subjected to three successive uniaxial compression tests up to a maximum strain of 90% compression. The mechanical cycles were irreversible and the hysteresis energy U_{hys} was much lower as compared to the gel samples after preparation state (Figs. S3 and S4). For instance, at C_o = 10%, U_{hys} decreases from 1.3 to 0.7 kJ m^{-3} as the number of cycles increases, as compared to 3 ± 0.3 kJ m^{-3} for the same gel after its preparation. The loss of energy dissipation mechanism upon swelling in water was also reflected by tensile mechanical tests. The dashed curves in Fig. 3 representing stress–strain data of swollen gel samples reveal that, upon removal of the surfactant, high stretchable PNIPAAm gel becomes a brittle one and ruptures at a stretch of λ_f = 4.0 ± 0.1 and 2.5 ± 0.1 for C_o = 10% and 15%, respectively (Fig. 3). The loss of the energy dissipation within the gel network after swelling thus deteriorates the mechanical performance of hydrogels. In accord with these results, the swollen hydrogel samples have no self-healing abilities.

Thus, PNIPAAm hydrogels have the ability to self-heal as long as they contain surfactant micelles, which hinder their use in aqueous environments. Consequently, the question arises how to fix the surfactant micelles within the gel network in aqueous solutions? Previous work shows that polymer systems containing bound surfactant micelles could be generated from hydrophobically modified polyelectrolytes with oppositely charged surfactants in aqueous solutions via hydrophobic and electrostatic interactions [50–59]. For instance, the interactions between hydrophobically modified polyacrylic acid (PAAc) with CTAB in aqueous solutions are known to result in complexation so that the surfactant remains bounded in the polymer coil.

To fix CTAB within the physical PNIPAAm network, we replaced half of the NIPAAm units of PNIPAAm hydrogels with acrylic acid (AAc) ones. For this purpose, the micellar copolymerization of equimolar amounts of NIPAAm and AAc together with 2 mol% C18 was carried out at C_o = 15% in aqueous CTAB solutions. CTAB concentrations in the reaction solution were 5% and 10%. All the physical gels consisting of poly(NIPAAm-AAc) network chains formed after a reaction time of 24 h were insoluble in water with a gel fraction close to unity, revealing that both the monomers AAc and NIPAAm as well as C18 are incorporated completely into the physical network.

The filled symbols in Fig. 9A show the relative mass (m_{rel}) of poly(NIPAAm-AAc) hydrogels plotted against the swelling time in water. For comparison, the data obtained from pure PNIPAAm hydrogels are also shown by open symbols. It is seen that, after incorporation of AAc units into the polymer, the swelling profile of the resulting hydrogels drastically changes; they exhibit no more maxima and the equilibrium swelling degree decreases from 3.4 ± 0.3 to 1.85 ± 0.05. Increasing CTAB content of the reaction solution from 5% to 10% results in deswelling of the hydrogels in water with 54% reduction in the gel mass. The results thus indicate the onset of complexation between AAc units and CTAB upon immersion in water, whose extent increases with increasing amount of CTAB at the gel preparation. Indeed, poly(NIPAAm-AAc) hydrogels were opaque both after preparation and after equilibrium in water indicating formation of a two-phase structure. As seen in Fig. 9B, equilibrium swollen poly(NIPAAm-co-AAc) hydrogels exhibit, although to a lesser extent than PNIPAAm hydrogels (Fig. 7B), temperature sensitivity. A broad deswelling transition occurs at around 30 °C with 28–34% reduction in the water content of the hydrogels.

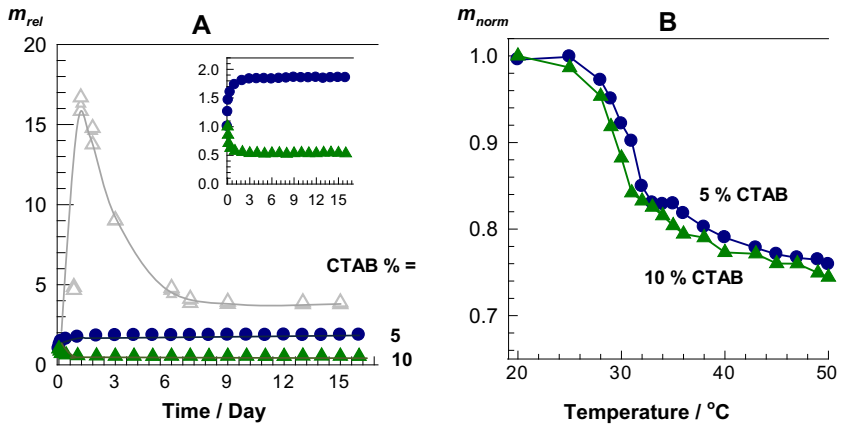

Fig. 9. (A): Relative mass m_{rel} of poly(NIPAAm-AAc) hydrogels plotted against the swelling time in water. For comparison, the data obtained from pure PNIPAAm hydrogels are shown by open symbols. The inset is a zoom-in of the graphic. (B): The mass m_{norm} of the hydrogels equilibrium swollen in water plotted against the temperature. The masses of the gel samples were normalized with respect to those at 24 °C.

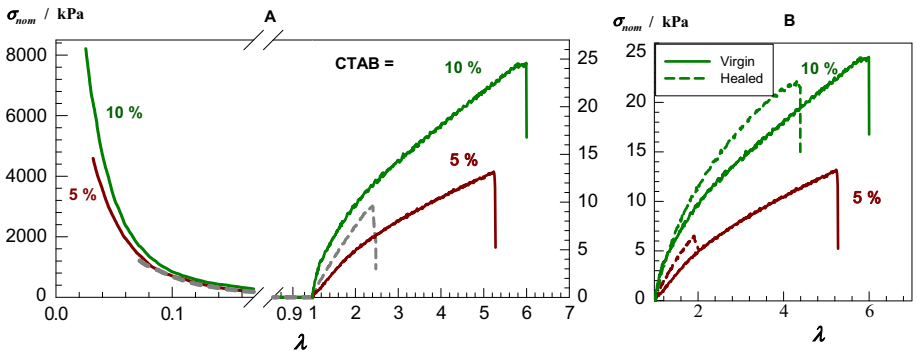

Fig. 10. (A): Stress–strain curves of poly(NIPAAm-AAc) hydrogels under compression and elongation. The hydrogels are equilibrium swollen in water. The gray dashed curves represent data obtained from swollen PNIPAAm hydrogels. (B): Stress–strain curves of virgin (solid) and healed swollen poly(NIPAAm-AAc) hydrogel samples (dashed). CTAB contents at the preparation state are indicated. Temperature = 24 °C.

To highlight the effect of polymer-bound CTAB on the mechanical properties of the hydrogels, cylindrical gel samples after a reaction time of 24 h were subjected to uniaxial elongation and compression tests. Fig. 10A represents stress–strain data of poly(NIPAAm-AAc) hydrogels in equilibrium with water (solid curves). For comparison, the data of swollen PNIPAAm hydrogels are also shown by the dashed gray curves. A significant improvement in the mechanical performance of hydrogels is observable upon addition of AAc units in the network chains. With 10% CTAB in the reaction feed, poly(NIPAAm-AAc) hydrogels equilibrium swollen in water sustain 24 ± 3 kPa stresses at a stretch λ_f of 5 ± 1 while, without AAc units, they break under 9 ± 2 kPa stresses at $\lambda_f = 2 \pm 1$. Such a change in the mechanical properties of hydrogels is attributed to the complex formation between CTA counterions and AAc anions of polymer. Poly(NIPAAm-AAc) hydrogels were also subjected to healing tests under various healing conditions. Although autonomic self-healing was not observed, increasing the healing temperature and treatment of the cut surfaces with acid or surfactant solutions provided healing in damaged gel samples. The highest healing efficiencies were achieved when the cut surfaces were treated for 1 h at 35 °C with 10% CTAB solutions of pH = 1. This treatment seems to provide dissolution of PAAc-CTAB complex in the damaged area. Then, the cut surfaces were pressed together and held at 80 °C for 1 h, following swelling in water to remove surfactant and acid. The hydrogels prepared in both 5% and 10% CTAB solutions could be healed after this treatment. Fig. 10B shows stress–strain curves of the virgin (solid curves) and healed gel samples (dashed curves) in equilibrium with water. The healed hydrogel sample formed in 10% CTAB sustains 22 ± 2 kPa stresses at a stretch of 4.2 ± 1.2, indicating a healing efficiency of around 80%. Thus, after introducing AAc units into PNIPAAm chains, self-healing PNIPAAm hydrogels in equilibrium with water could be generated.

4. Conclusions

In this study, we described preparation of PNIPAAm hydrogels with autonomous self-healing ability. Strong hydrophobic interactions were used to physically crosslink PNIPAAm chains in a micellar solution. The hydrogels were prepared by

micellar copolymerization of NIPAAm with 2 mol% C18 in 0.25 M NaBr solution of CTAB. The as-prepared PNIPAAm hydrogels exhibit frequency-dependent dynamic moduli and a loss factor above 0.1 due to the temporary nature of the hydrophobic associations in the presence of CTAB micelles. Cyclic mechanical tests show significant mechanical hysteresis and reversible loading/unloading cycles up to large maximum strains indicating that the damage done to the gel samples during the loading is recoverable in nature. The hydrogels indeed have autonomous self-healing ability with an efficiency of up to 100% as evidenced by mechanical measurements. However, the hydrogels undergo a significant change in their internal dynamics upon swelling in water, i.e., after extraction of CTAB micelles, and lose their ability to self-heal. This structural change occurs due to the strengthening of hydrophobic associations in the absence of CTAB. By incorporating acrylic acid (AAc) units within the supramolecular PNIPAAm network, self-healing in swollen PNIPAAm hydrogels is achieved due to the fixing of CTAB in the gel phase by complexation with AAc units.

Acknowledgments

Work was supported by the Scientific and Technical Research Council of Turkey (TUBITAK), KBAG 114Z312. OO thanks the Turkish Academy of Sciences (TUBA) for the partial support.

Appendix A. Supplementary material

Supplementary data associated with this article can be found, in the online version, at http://dx.doi.org/10.1016/j.eurpolymj.2015.09.002.

References

[1] Y. Hirokawa, T. Tanaka, Volume phase transition in a nonionic gel, J. Chem. Phys. 81 (1984) 6379–6380.
[2] S. Hirotsu, Coexistence of phases and the nature of first-order transition in poly(N-isopropylacrylamide) gels, Adv. Polym. Sci. 110 (1993) 1–26.
[3] Y.H. Bae, T. Okano, R. Hsu, S.W. Kim, Thermo-sensitive polymers as on-off switches for drug release, Macromol. Chem. Rapid Commun. 8 (1987) 481–485.
[4] L.C. Dong, A.S. Hoffman, Thermally reversible hydrogels III Immobilization of enzymes for feedback reaction control, J. Control. Release 4 (1986) 223–227.
[5] T.G. Park, A.S. Hoffman, Immobilization and characterization of b-galactosidase in thermally reversible hydrogel beads, J. Biomed. Mater. Res. 21 (1990) 24–32.
[6] R.F.S. Freitas, E.L. Cussler, Temperature sensitive gels as extraction solvents, Chem. Eng. Sci. 41 (1987) 97–105.
[7] C. Park, I. Orozco-Avila, Concentrating cellulases from fermented broth using a temperature-sensitive hydrogel, Biotechnol. Prog. 8 (1992) 521–526.
[8] I. Galaev, B. Mattiasson, Smart Polymers. Applications in Biotechnology and Biomedicine, CRC Press, NY, 2008.
[9] S.H. Gehrke, G.P. Andrews, E.L. Cussler, Chemical aspects of gel extraction, Chem. Eng. Sci. 41 (1986) 2153–2160.
[10] N. Kayaman, D. Kazan, A. Erarslan, O. Okay, B.M. Baysal, Structure and protein separation efficiency of poly(N-isopropylacrylamide) gels: effect of synthesis conditions, J. Appl. Polym. Sci. 67 (1998) 805–814.
[11] P. Fratzl, Biomimetic materials research: what can we really learn from nature's structural materials?, J R. Soc. Interf. 4 (2007) 637–642.
[12] A.R. Hamilton, N.R. Sottos, S.R. White, Self-healing of internal damage in synthetic vascular materials, Adv. Mater. 22 (2010) 5159–5163.
[13] G.E. Fantner, E. Oroudjev, G. Schitter, L.S. Golde, P. Thurner, M.M. Finch, P. Turner, T. Gutsmann, D.E. Morse, H. Hansma, P.K. Hansma, Sacrificial bonds and hidden length: Unraveling molecular mesostructures in tough materials, Biophys. J. 90 (2006) 1411–1418.
[14] M.D. Hager, P. Greil, C. Leyens, S. van der Zwaag, U.S. Schubert, Self-healing materials, Adv. Mater. 22 (2010) 5424–5430.
[15] N.K. Guimard, K.K. Oehlenschlaeger, J. Zhou, S. Hilf, F.G. Schmidt, C. Barner-Kowollik, Current trends in the field of self-healing materials, Macromol. Chem. Phys. 213 (2012) 131–143.
[16] D.Y. Wu, S. Meure, D. Solomon, Self-healing polymeric materials: a review of recent developments, Prog. Polym. Sci. 33 (2008) 479–522.
[17] X. Zhao, Multi-scale multi-mechanism design of tough hydrogels: building dissipation into stretchy networks, Soft Matter. 10 (2014) 672–687.
[18] Y. Zhao, F. Sakai, L. Su, Y. Liu, K. Wei, G. Chen, M. Jiang, Progressive macromolecular self-assembly: from biomimetic chemistry to bio-inspired materials, Adv. Mater. 25 (2013) 5215–5256.
[19] A.B.W. Brochu, S.L. Craig, W.M. Reichert, Self-healing biomaterials, J. Biomed. Mater. Res. A 96 (2011) 492–506.
[20] Y. Yang, M.W. Urban, Self-healing polymeric materials, Chem. Soc. Rev. 42 (2013) 7446–7467.
[21] R.P. Wool, Self-healing materials: a review, Soft Matter. 4 (2008) 400–418.
[22] Z. Wei, J.H. Yang, J. Zhou, F. Xu, M. Zrinyi, P.H. Dussault, Y. Osada, Y.M. Chen, Self-healing gels based on constitutional dynamic chemistry and their potential applications, Chem. Soc. Rev. 43 (2014) 8114–8131.
[23] S. Seiffert, J. Sprakel, Physical chemistry of supramolecular polymer networks, Chem. Soc. Rev. 41 (2012) 909–930.
[24] T. Rossow, S. Seiffert, Supramolecular polymer networks: preparation, properties, and potential, Adv. Polym. Sci. 268 (2015) 1–46.
[25] A. Phadke, C. Zhang, B. Arman, C.-C. Hsu, R.A. Mashelkar, A.K. Lele, M.J. Tauber, G. Arya, S. Varghese, Rapid self-healing hydrogels, PNAS 109 (2012) 4383–4388.
[26] J. Liu, G. Song, C. He, H. Wang, Self-healing in tough graphene oxide composite hydrogels, Macromol. Rapid Commun. 34 (2013) 1002–1007.
[27] K. Haraguchi, K. Uyama, H. Tanimoto, Self-healing in nanocomposite hydrogels, Macromol. Rapid Commun. 32 (2011) 1253–1258.
[28] J.-Y. Sun, X. Zhao, W.R.K. Illeperuma, O. Chaudhuri, K.H. Oh, D.J. Mooney, J.J. Vlassak, Z. Suo, Highly stretchable and tough hydrogels, Nature 489 (2012) 133–136.
[29] E.A. Appel, F. Biedermann, U. Rauwald, S.T. Jones, J.M. Zayed, O.A. Scherman, Supramolecular cross-linked networks via host–guest complexation with cucurbit[8]uril, J. Am. Chem. Soc. 132 (2010) 14251–14260.
[30] Z. Shafiq, J. Cui, L. Pastor-Perez, V. San Miguel, R.A. Gropeanu, C. Serrano, A. del Campo, Bioinspired underwater bonding and debonding on demand, Angew. Chem. Int. Ed. 124 (2012) 4408–4411.
[31] Y. Xu, Q. Wu, Y. Sun, H. Bai, G. Shi, Three-dimensional self-assembly of graphene oxide and DNA into multifunctional hydrogels, ACS Nano. 4 (2010) 7358–7362.
[32] F. Liu, F. Li, G. Deng, Y. Chen, B. Zhang, J. Zhang, C.-Y. Liu, Rheological images of dynamic covalent polymer networks and mechanisms behind mechanical and self-healing properties, Macromolecules 45 (2012) 1636–1645.
[33] P. Froimowicz, D. Klinger, K. Landfester, Photoreactive nanoparticles as nanometric building blocks for the generation of self-healing hydrogel thin films, Chem. Eur. J. 17 (2011) 12465–12475.
[34] O. Okay, Self-healing hydrogels formed via hydrophobic interactions, Adv. Polym. Sci. 268 (2015) 101–142.

[35] T. Wang, S. Zheng, W. Sun, X. Liu, S. Fu, Z. Tong, Notch sensitive and self-healing PNIPAm-PAM-clay nanocomposite hydrogels, Soft Matter. 10 (2014) 3506–3512.
[36] M. Chiper, D. Fournier, R. Hoogenboom, U.S. Schubert, Thermosensitive and switchable terpyridine-functionalized metallo-supramolecular poly(N-isopropylacrylamide), Macromol. Rapid Commun. 29 (2008) 1640–1647.
[37] Y. Guan, H.-B. Zhao, L.-X. Yu, S.-C. Chen, Y.-Z. Wang, Multi-stimuli sensitive supramolecular hydrogel formed by host–guest interaction between PNIPAM-Azo and cyclodextrin dimers, RSC Adv. 4 (2014) 4955–4959.
[38] T. Rossow, S. Hackelbusch, P. van Assenbergh, S. Seiffert, A modular construction kit for supramolecular polymer gels, Polym. Chem. 4 (2013) 2515–2527.
[39] D.C. Tuncaboylu, M. Sari, W. Oppermann, O. Okay, Tough and self-healing hydrogels formed via hydrophobic interactions, Macromolecules 44 (2011) 4997–5005.
[40] D.C. Tuncaboylu, M. Sahin, A. Argun, W. Oppermann, O. Okay, Dynamics and large strain behavior of self-healing hydrogels with and without surfactants, Macromolecules 45 (2012) 1991–2000.
[41] G. Akay, A. Hassan-Raeisi, D.C. Tuncaboylu, N. Orakdogen, S. Abdurrahmanoglu, W. Oppermann, O. Okay, Self-healing hydrogels formed in catanionic surfactant solutions, Soft Matter. 9 (2013) 2254–2261.
[42] U. Gulyuz, O. Okay, Self-healing polyacrylic acid hydrogels, Soft Matter. 9 (2013) 10287–10293.
[43] M.P. Algi, O. Okay, Highly stretchable self-healing poly(N, N-dimethylacrylamide) hydrogels, Eur. Polym. J. 59 (2014) 113–121.
[44] U. Gulyuz, O. Okay, Self-healing poly(acrylic acid) hydrogels with shape memory behavior of high mechanical strength, Macromolecules 47 (2014) 6889–6899.
[45] A. Chetty, J. Kovacs, Z. Sulyok, A. Meszaros, J. Fekete, A. Domjan, A. Szilagyi, V. Vargha, A versatile characterization of poly(N-isopropylacrylamide-co-N, N′-methylene-bis-acrylamide) hydrogels for composition, mechanical strength, and rheology, Exp. Polym. Lett. 7 (2013) 95–105.
[46] G.L. Puleo, F. Zulli, M. Piovanelli, M. Giordano, B. Mazzolai, L. Beccai, L. Andreozzi, Mechanical and rheological behavior of pNIPAAM crosslinked macrohydrogel, React. Funct. Polym. 73 (2013) 1306.
[47] E. Volpert, J. Selb, F. Candau, Associating behaviour of polyacrylamides hydrophobically modified with dihexylacrylamide, Polymer 39 (1998) 1025–1033.
[48] S. Biggs, J. Selb, F. Candau, Copolymers of acrylamide and N-alkylacrylamide in aqueous solution: the effects of hydrolysis on hydrophobic interactions, Polymer 34 (1993) 580–591.
[49] R.E. Webber, C. Creton, H.R. Brown, J.P. Gong, Large strain hysteresis and Mullins effect of tough double-network hydrogels, Macromolecules 40 (2007) 2919–2927.
[50] P.F.C. Lim, L.Y. Chee, S.B. Chen, B.-H. Chen, Study of interaction between cetyltrimethylammonium bromide and poly(acrylic acid) by rheological measurements, J. Phys. Chem. B 107 (2003) 6491–6496.
[51] K. Yoshida, P.L. Dubin, Complex formation between polyacrylic acid and cationic/nonionic mixed micelles: effect of pH on electrostatic interaction and hydrogen bonding, Colloids Surf. A Physicochem. Eng. Aspects 147 (1999) 161–167.
[52] P. Ilekti, L. Piculell, F. Tournilhac, B. Cabane, How to concentrate an aqueous polyelectrolyte/surfactant mixture by adding water, J. Phys. Chem. B 102 (1998) 344–351.
[53] J. Fundin, P. Hansson, W. Brown, I. Lidegran, Poly(acrylic acid) – cetyltrimethylammonium bromide interactions studied using dynamic and static light scattering and time-resolved fluorescence quenching, Macromolecules 30 (1997) 1118–1126.
[54] J.O. Carnali, (Polymer/polymer)-like phase behavior in the system tetradecyltrimethylammonium bromide/sodium polyacrylate/water, Langmuir 9 (1993) 2933–2941.
[55] L. Chiappisi, I. Hoffmann, M. Gradzielski, Complexes of oppositely charged polyelectrolytes and surfactants – recent developments in the field of biologically derived polyelectrolytes, Soft Matter. 9 (2013) 3896–3909.
[56] P. Hansson, Self-assembly of ionic surfactant in cross-linked polyelectrolyte gel of opposite charge. A physical model for highly charged systems, Langmuir 14 (1998) 2269–2277.
[57] C. Wang, K.C. Tam, New insights on the interaction mechanism within oppositely charged polymer/surfactant systems, Langmuir 18 (2002) 6484–6490.
[58] B. Magny, I. Iliopoulos, R. Zana, R. Audebert, Mixed micelles formed by cationic surfactants and anionic hydrophobically modified polyelectrolytes, Langmuir 10 (1994) 3180–3187.
[59] O.E. Philippova, D. Hourdet, R. Audebert, A.R. Khokhlov, Interaction of hydrophobically modified poly(acrylic acid) hydrogels with ionic surfactants, Macromolecules 29 (1996) 2822–2830.